Principles and Performance of Traveling-Wave Photodetector Arrays

Charles L. Goldsmith, *Senior Member, IEEE,* Gregory A. Magel, *Member, IEEE,* and Richard J. Baca, *Member, IEEE*

***Abstract*—Analog fiber-optic links are used in a variety of microwave applications, including cable-TV and cellular-telephone distribution, as well as antenna remoting. The RF insertion loss and output power obtainable from externally modulated links is primarily limited by photodetector optical-power handling capabilities. Using traveling-wave concepts similar to those in microwave distributed amplifiers, we demonstrate the principle of traveling-wave detector arrays (TWDA's) in which discrete photodiodes are embedded within an artificial transmission line. By feeding these detectors with suitably time-delayed optical signals, this arrangement coherently combines multiple RF photocurrents into a single output. This paper presents the theory, construction details, and results of two- and four-element TWDA's operating up into the Ku-band. We demonstrate a two-element TWDA yielding a 6-dB improvement in insertion loss and RF output power with 12 GHz of operating bandwidth, and a four-element TWDA yielding 12-dB improvement up to 18 GHz.**

***Index Terms*— Traveling wave, photodetector, photodetector array, artificial transmission line, p-i-n photodiodes, microwave, analog fiber-optic links, high illumination, optical-power handling.**

I. Introduction

HIGH-PERFORMANCE analog fiber-optic links, which operate at microwave frequencies, commonly use low-noise high-power lasers and external intensity modulators. Improvements in the RF insertion loss of these links require either more sensitive modulators or higher modulated optical-power levels at the detector. Since the detection process converts a modulated optical carrier into RF current, the RF output power is proportional to the square of the modulated optical power. With the advent of high-power diode-pumped solid-state lasers (with $>$100 mW output power), the potential improvements in insertion loss of these links is currently limited by photodetector optical-power handling. Detectors used in microwave applications must be designed for small capacitance, and hence, small diameters in order to operate at microwave frequencies. To increase optical-power handling capability, it is necessary to either increase the area of the detector (at the cost of higher capacitance and reduced bandwidth), optimize the design of the photodetector geometry or epitaxy, or combine the photocurrents from several detectors.

In this paper, we discuss a concept for combining the photocurrents from a multiplicity of individual photodetector elements. This concept is commonly used in microwave distributed amplifiers, and can be used with photodetectors to create a structure we call the traveling-wave detector array (TWDA). The TWDA embeds several microwave-speed optical detectors within a quasi-transmission-line structure which coherently combines their RF photocurrents while retaining their high RF bandwidth. This artificial transmission line is designed for a 50-Ω characteristic impedance by balancing the detector capacitances with appropriate series inductances. The optical signal is distributed to the photodetectors in the proper RF phase by tailored-length optical fibers. These fibers are constructed such that the electrical signal delay between detectors is matched by the optical delay between the fibers. We report the demonstration of two-detector and four-detector TWDA's operating at frequencies as high as 18 GHz. This photocurrent combining technique promises improvement in optical-power handling which scales roughly with the number of detectors.

Traveling-wave concepts have been applied to improving photodetector bandwidth and power handling by several authors in the recent literature [1]–[6]. Giboney *et al.* [2], [3] and Hietala *et al.* [4] demonstrated single-element traveling-wave photodetectors in which the distribution of the detector capacitance along the transmission-line electrodes removes the conventional area-bandwidth constraint. Wu *et al.* [5], [6] placed detectors serially along a semiconductor waveguide and tailored the microwave interconnection network for proper delays to coherently combine the photocurrents of several detectors. The work reported here differs from previous work in two respects. First, the detector elements are disposed serially along a microwave transmission line and are fed by a properly delayed parallel passive optical network. This allows all detectors to receive the same optical power. With serial optical feeds, the optical-power handling of the network is limited by that of the first detector, and all subsequent detectors are underutilized. Second, our technique allows the use of normally illuminated detectors for high coupling efficiency. To the best of our knowledge, this paper is the first to apply traveling-wave concepts using commercially available photodetectors. This technique could be used in conjunction with any detector elements, including future high-power photodetectors.

II. Principles of Operation

Most commercially available photodetector circuits consist of a single detector connected in an impedance-matched system, as shown in Fig. 1. A typical detector module consists of a single detector resistively matched with a 50-Ω termina-

Manuscript received December 4, 1996; revised May 12, 1997.

The authors are with Texas Instruments Incorporated, Dallas, TX, 75265 USA.

Publisher Item Identifier S 0018-9480(97)06009-2.

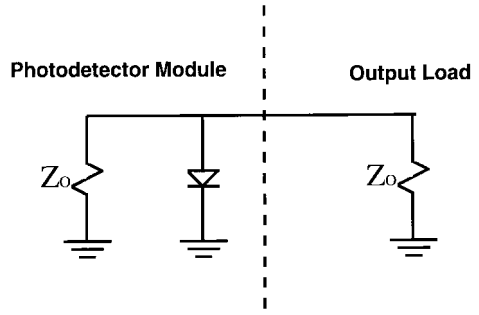

Fig. 1. Simple photodetector module schematic using resistively matched photodiode.

tion resistor. The termination resistor establishes a relatively good load impedance looking back into the detector module. This prevents impedance mismatches from the open-circuit impedance of the detector from causing excessive ripple in the transmission response of the detector network. Bias circuitry is commonly included to bias the detector while decoupling the dc voltage from the output and the termination (*not* shown in Fig. 1 for simplicity). The signal current from the detector divides according to the two load resistors, resulting in half the signal current being delivered to the output load. This inefficiency allows impedance-matched operation, yielding a flat detector response over very broad bandwidths. The bandwidth of this detector network is fundamentally limited by the transit time of the carriers within the detector and the *RC* time constant of the detector junction capacitance/load impedances. Generally, photodetectors with bandwidths less than 20 GHz are designed such that the transit time is not a limitation, and their bandwidth is *RC* limited. The cutoff frequency f_c of the detector response is given as

$$f_c = \frac{1}{\pi Z_o C_d}$$

where C_d is the detector junction capacitance and Z_o the matched load impedance.

The simplest approach to combining the signals from several photodetectors is to connect them in parallel. With this arrangement, the detector currents add in phase, but so does the capacitance of the individual detectors. Therefore, an arrangement of N detectors will produce N times the current, but have a total capacitance of N times the individual junction capacitance. This leads to a bandwidth $1/N$ times that of a single detector.

An alternative method for building a multielement detector is to use traveling-wave techniques commonly employed in the design of distributed amplifiers. Individual detector capacitances can be kept from adding together by embedding them within an artificial transmission line where the detectors are interconnected with inductors, as shown in Fig. 2. Every section of this detector array, consisting of two inductors and the detector junction capacitance, operates similar to an m-derived filter section. The cascade of these filter sections produces a ladder network which closely resembles the lumped-element approximation to a transmission line. The characteristic impedance of this artificially constructed transmission line, Z_a, is given by the ratio of inductance to

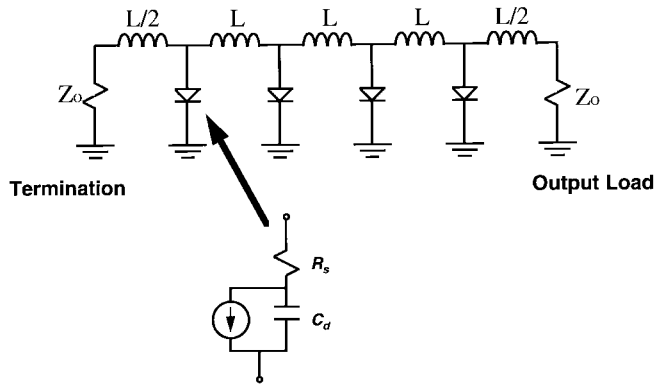

Fig. 2. Schematic of traveling-wave photodetector array. Photodiodes are interconnected with proper inductances to yield an artificial transmission line of impedance Z_o.

capacitance

$$Z_a = \sqrt{\frac{L}{C_d}}$$

where L is the total inductance per filter section. Meanwhile, the cutoff frequency of this network, is determined by

$$f_c = \frac{1}{\pi\sqrt{LC_d}}.$$

While the junction capacitances no longer add together, the individual RF photocurrents are now separated by the time delay of the m-derived filter sections. This electrical propagation delay, τ_e, is nominally given by

$$\tau_e \approx \sqrt{LC_d}$$

and is valid for frequencies well below the cutoff-frequency f_c.

Once the individual detectors are connected such that their output currents can be added without reducing the overall circuit bandwidth, it is possible to coherently drive the detectors using an appropriate optical-feed network. This feed network must provide the proper optical delays such that all signal paths experience the same total propagation delay. A schematic diagram of such a network is shown in Fig. 3. In this network, an optical input power level P_{opt} is split into N outputs, with each having P_{opt}/N output optical power. The optical time delay between each set of outputs is τ_o. Every output signal is demodulated by a photodetector of responsivity η, creating a current in each detector. These photocurrents split in half, traveling in two directions—toward both the termination and the output load. The current traveling to the output port from a given detector, I_n, is given by

$$I_n = e^{j(n-1)\omega\tau_o} \cdot \frac{\eta P_{\text{opt}}}{2N} \cdot e^{j(N-n)\omega\tau_e}$$

where ω is the microwave frequency of the signal, τ_o is the optical delay between outputs, η is the responsivity of the detector, P_{opt} is the optical input power, N is the number of detector outputs, and τ_e is the electrical delay between each detector. The first term of the above equation is the relative optical delay to the detector, the second is the magnitude of the photocurrent generated, and the third term is the electrical

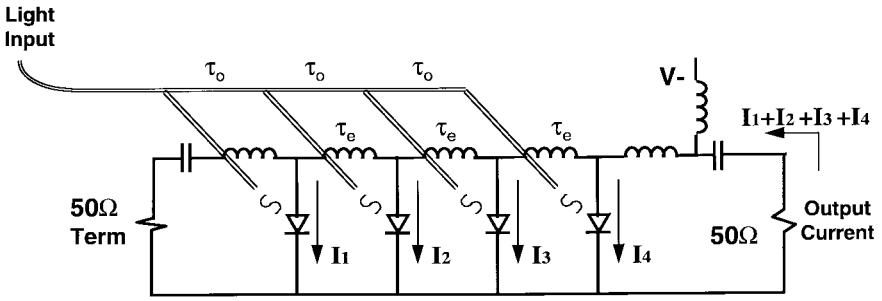

Fig. 3. Complete diagram of TWDA. Optical signals experience progressive delays of τ_o while electrical signals experience progressive delays of τ_e. Proper phasing of optical and electrical signals causes photocurrents to add in-phase at the output load resistor.

delay between the photodetector and the output. The sum of all the photocurrents at the output I_o is

$$I_o = \sum I_n = \sum_{n=1}^{N} \left[e^{j(n-1)\omega\tau_o} \cdot \frac{\eta P_{\text{opt}}}{2N} \cdot e^{j(N-n)\omega\tau_e} \right].$$

For the RF photocurrents of the detectors to add coherently, it is necessary for the optical delays between outputs to be equal to the electrical delays between detectors. This can be simply accomplished by using a fiber or waveguide feed network that has longer paths toward the output of the detector array. Making the optical delays of the feed network equal to the electrical-network propagation delays

$$\tau_o = \tau_e = \tau$$

yields

$$I_o = \sum_{N} I_n = \frac{\eta P_{\text{opt}}}{2} \cdot e^{j(N-1)\omega\tau}$$

as the total RF output current. By coherently combining the RF photocurrents at the output of the detector array, a total current is obtained which is N times that which would be obtained with a single detector in a matched impedance network.

A. Microwave Networks

When building electrical networks at microwave frequencies, ideal inductors are commonly approximated with short lengths of high-impedance transmission line. To facilitate this, the individual interconnecting inductors between detectors are replaced by high-impedance transmission lines of impedance Z_L and effective propagation index n_L. A schematic of this network is shown in Fig. 4. Picking the length of the transmission-line section d_L to yield the desired traveling impedance $Z_a = Z_o$ requires [7]

$$d_L = \frac{cZ_L C_d}{\left[\frac{Z_L^2}{Z_o^2} - 1\right] n_L}.$$

This network has an effective propagation index of

$$n_a = \frac{Z_L n_L}{Z_o}$$

and, therefore, a propagation delay between individual detectors of

$$\tau_e = \frac{Z_L^2 C_d}{\left[\frac{Z_L^2}{Z_o^2} - 1\right] Z_o}.$$

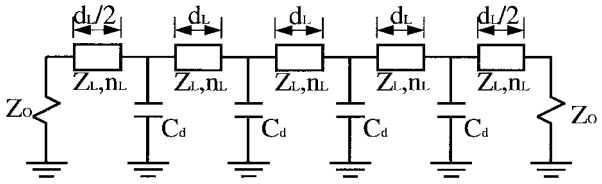

Fig. 4. TWDA concept using short lengths of high-impedance transmission line instead of ideal inductors.

This yields a cutoff frequency of

$$f_c = \frac{1}{Z_o \pi C_d}\left[1 - \frac{Z_o^2}{Z_L^2}\right] = \frac{1}{\pi\tau_e}.$$

Utilizing sections of transmission line instead of bondwire inductors creates a network with much more repeatable and controllable characteristics. On many occasions, bondwires are used as inductors in networks which operate below 10 GHz. However, circuits which operate above 10 GHz are generally more sensitive to bondwire inductance variations and use semidistributed networks as described above.

III. TWDA's

Two different TWDA's were constructed and tested to determine the feasibility of this concept. First, a simple two-element array was constructed which operated up to 12 GHz. Secondly, a more sophisticated four-element array was constructed which operated up to 18 GHz.

A. Two-Element TWDA Construction

Fig. 5 shows a photomicrograph of a two-element TWDA constructed using two commercially available 75-μm-diameter back-illuminated InGaAs p-i-n photodiodes (Lasertron QDE-075C). Each photodiode is specified to operate to at least 10 GHz, and is mounted on an alumina submount with clearance hole access to the backside for fiber coupling.

The p-i-n photodetectors were characterized using the De-Loach technique [8], yielding a junction capacitance of 0.5 pF and a series resistance of approximately 5 Ω. The series inductors for this demonstration were implemented using interconnecting bondwires. Each bondwire was fabricated with a length of approximately 1 mm. This is equivalent to $\sim$ 0.6 nH, which yields an artificial transmission-line impedance of $Z_o = (L/C)^{1/2} = 50\,\Omega$. These bondwires also connect the detectors to input and output alumina 50-Ω microstrip transmission

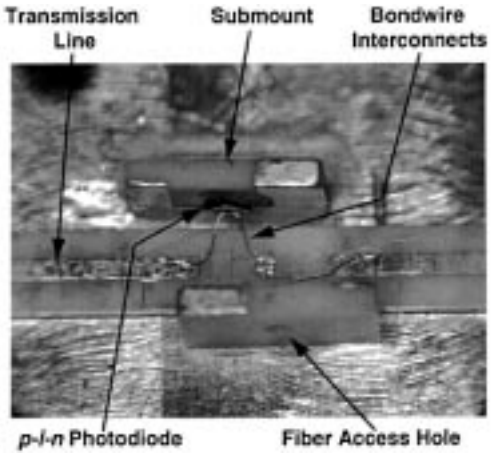

Fig. 5. Close-up photo of two-element TWDA.

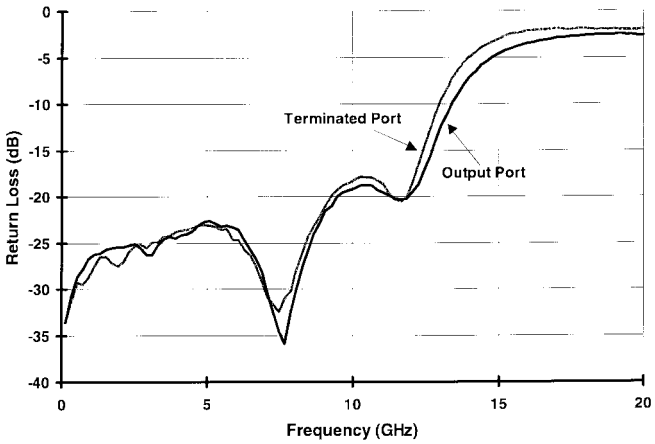

Fig. 6. Microwave match characteristics (return loss) of two-element TWDA at 5-V reverse bias. Return loss is shown for both ports of the detector array.

lines in a 20-GHz microwave test fixture. The tuning of the bondwires is not critical, since sensitivity to element values is relatively low in passive filter networks of this type. Wiltron K-connectors provide RF connections to the input termination and output load.

Optical fibers were aligned using multiaxis positioning stages from either side of the microwave test fixture, and adjusted for roughly equal coupling efficiency. Alignment is relatively uncritical due to the large size of the surface-illuminated photodiodes. Custom photodiode submounts could be used to fix the fibers in place after alignment, allowing a more permanent mounting as well as being more suitable for connecting a large number of fibers and detectors.

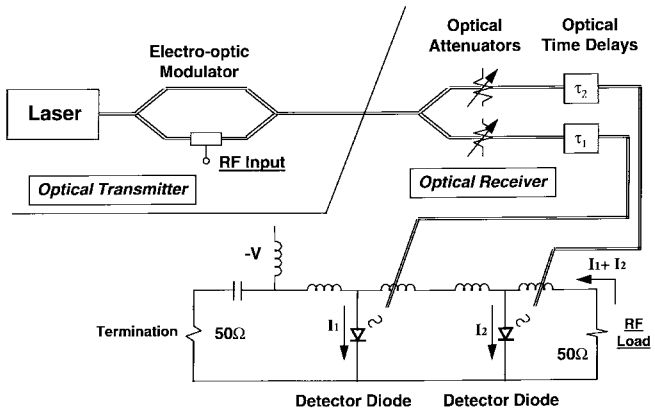

Fig. 7. Schematic of fiber-optic link utilizing a TWDA.

B. Two-Element TWDA Results

Measured return-loss characteristics of the photodiode array (with no optical input) are shown in Fig. 6. A reverse bias of 5 V was applied to the photodiodes through the internal bias tee of an HP 8720B vector network analyzer. The return loss of the artificial transmission line is $>$ 15 dB from 130 MHz to 12 GHz, indicating a good match to the desired 50-Ω characteristic impedance. The return loss at high frequencies degrades due to the cutoff of the artificial transmission line. This cutoff is determined by the interconnect inductance and photodiode capacitance. For the network described above, the cutoff is approximately 12 GHz, and is in good agreement with the theory.

Next, the setup shown in Fig. 7 was assembled to measure the performance of a fiber-optic link using the multielement detector. A 200-mW diode-pumped YAG laser at 1.3-μm wavelength was modulated using a $LiNbO_3$ integrated-optic modulator with a nominal electrical bandwidth of 12 GHz. The modulator was driven directly by the network analyzer. A 3-dB (1:2) fused fiber splitter divided the modulated light into two equal-intensity paths in single-mode optical fiber. Variable fiber attenuators and variable air-gap fiber delay lines were used to adjust individual intensity and delay at the detectors. The attenuators were adjusted to approximately equalize the photocurrents at both detectors. Detector responsivities of $>$ 0.8 A/W were obtained, and measurements were taken with a dc photocurrent of 6.7 and 6.9 mA in the two detectors (13.6 mA total for both detectors). The optical beams in the variable delay lines could be blocked to measure the response of individual photodiodes. The delays were adjusted to equalize the microwave insertion phase of the individual detectors. The microwave propagation delay difference between the two detectors was approximately 25 ps.

The measured fiber-optic link frequency response is shown in Fig. 8. The frequency response for each of the individual detectors in the array are shown. These individual detector responses are similar to the response from a single detector in an impedance-matched environment, as shown in Fig. 1. However, the insertion loss of the detector farthest from the output, detector 1, rolls off faster than that of detector 2. The signal from detector 1 experiences the loss of both detector resistances, whereas the signal from detector 2 experiences only one. The total photoresponse of the detector array is the sum of the individual photocurrents from each detector. With both detectors illuminated equally, the fiber-link insertion response improves by 6 dB, since doubling the photocurrent yields a quadrupling of RF output power. This is also shown in Fig. 8.

Detuning the differential fiber delay away from time coherence using the variable delay lines, or simply by swapping the two fibers to the detectors, produces a deep notch ($>$ 30 dB)

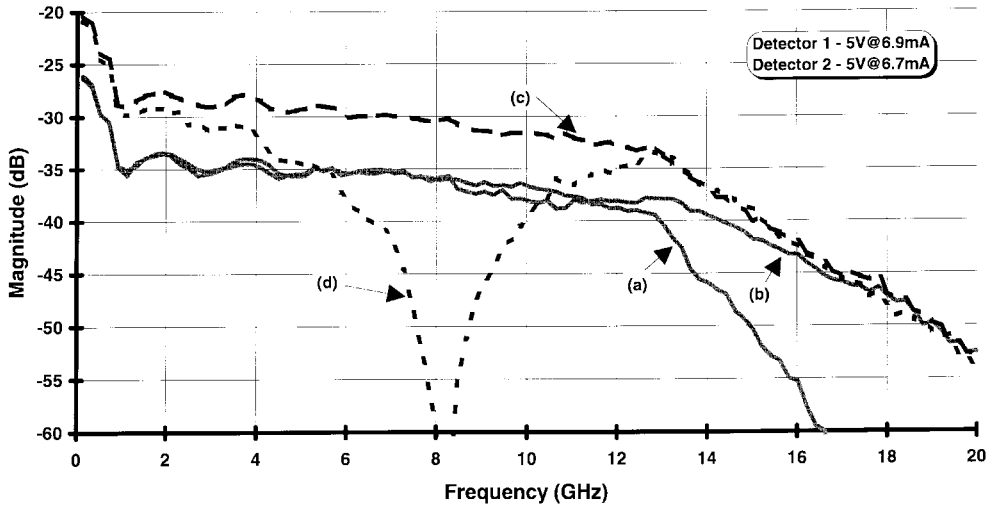

Fig. 8. Fiber-optic link insertion gain versus frequency for single detectors, detector 1: a, detector 2: b, and a two-detector TWDA with an optimum optical time delay: c. Link insertion loss for a two-detector TWDA with an additional 60 ps of optical time delay added between the two detector feeds: d. The frequency response ripples below 5 GHz are due to the modulator frequency response.

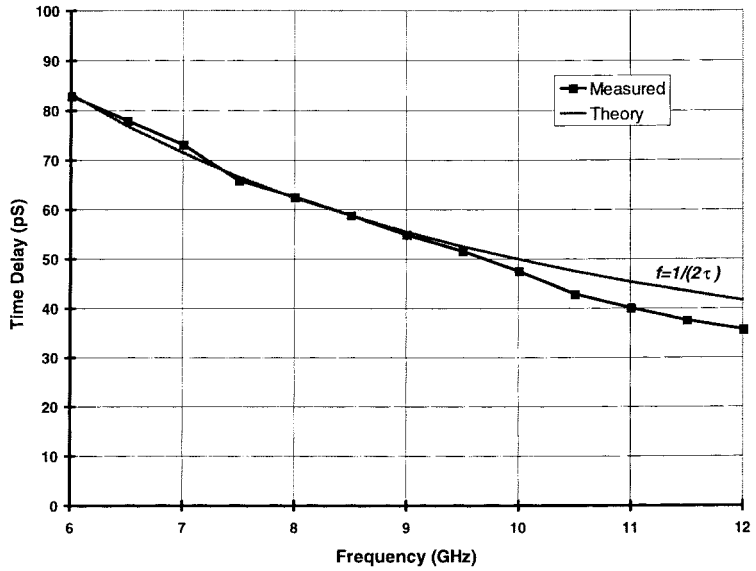

Fig. 9. Frequency of insertion response notch versus differential time delay added to the optical network.

in the frequency response. The notch occurs at a frequency proportional to the inverse of the differential delay detuning, $\Delta\tau$, given by

$$f_n = \frac{1}{2\Delta\tau}.$$

An example of this is shown in Fig. 8, where a 60-ps additional time delay has been added between the two fiber outputs. Measurements of the notch frequency as a function of additional time delay show an excellent match between predicted and measured frequencies, and is shown in Fig. 9. The theoretical and measured notch frequencies track until the cutoff frequency of the artificial transmission line—approximately 12 GHz in this network. Beyond the cutoff frequency, the transmission-line network becomes dispersive, having a varying time delay as a function of frequency. More general frequency-response tailoring is possible using delay detuning in multielement TWDA's. This could be used to create various bandpass and stopband filter responses while maintaining a broad-band RF output match on the TWDA.

Further improvements in link insertion loss are possible with higher laser power and better packaging. Separate compression measurements of photodetector response at 10 GHz have shown that these detector diodes can handle approximately 35 mW of optical power before the onset of compression. The two-element detector array could thus be illuminated with 70 mW of optical power for a photocurrent of approximately 60 mA. This would lead to significantly lower link insertion loss. Adding more photodiodes to the array would further increase optical-power handling up to the point at which voltage waves on the transmission line lead to the onset of nonlinearity in the detectors [9], [10]. Another limitation on the practical number of photodiodes is determined by the resistive component of the photodiode. As larger numbers

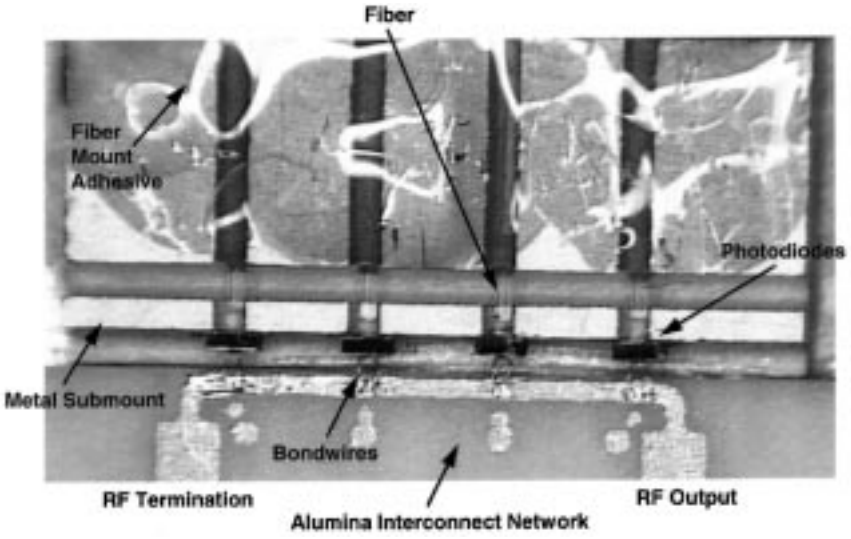

Fig. 10. Micrograph of a four-element TWDA build on a metal submount.

of photodiodes are incorporated, the resistive losses in the distributed network will cause a premature rolloff in the frequency response. For the detectors used in this experiment, it is estimated that at least four or eight photodiodes could be cascaded before the rolloff at 10 GHz becomes significant.

Improvements in packaging were made by replacing the variable delay lines and attenuators with custom cleaved fibers of the proper length difference (25 ps of delay) required to drive the TWDA coherently. A fiber delay length accuracy of 0.15 ps was achieved using an HP 8504B precision optical reflectometer, a custom fiber translation fixture, and a York FK11 ultrasonic cleaver. After optimizing and equalizing the detector coupling, this simpler configuration with reduced optical losses produced proportionately lower insertion losses. It is possible to envision using this technology in conjunction with high-power lasers to achieve fiber-link performance with lossless operation over broad bandwidths.

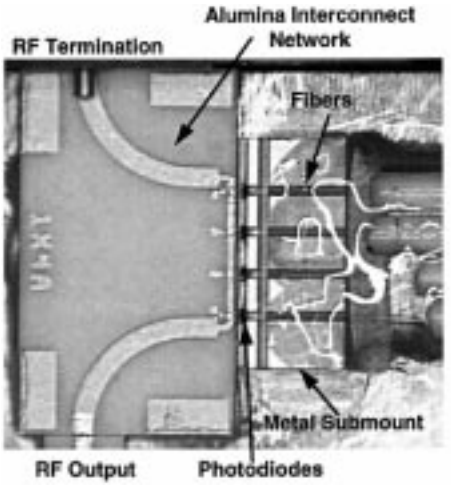

Fig. 11. Photograph of a complete four-element TWDA including electrical interconnect network and fiber feeds.

C. Four-Element TWDA Construction

Next, an improved TWDA was developed and tested with operation up to 18 GHz. The goals of this array were an increased number of detectors, replacement of bondwire tuning with a thick-film microwave circuit, and incorporation of higher frequency detectors with improved heatsinking.

This TWDA incorporated four Lasertron QDE-035C 35-μm-diameter p-i-n photodetectors rated for operation up to 18 GHz. The detectors were die attached with AuSn to a custom electro-discharge machined (EDMed) copper-moly submount. This gold plated submount acts as both a diode mount as well as a permanent fiber mount for aligning and cementing the fiber. A photograph of this submount and four-element detector array is shown in Fig. 10. Four EDMed channels perpendicular to the diode faces act as guides for fiber positioning and mounting. Precision machining of the four fiber channels allows precise positioning of the photodetectors relative to the microwave interconnect network. The channel parallel to the detector faces acted as a stop for the UV curing epoxy, keeping it from wicking down the channels and coming in contact with the photodetectors. The mechanical properties of the copper-moly used in the submount provides

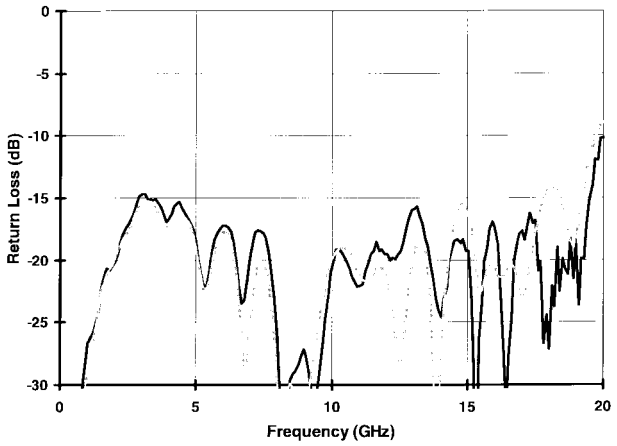

Fig. 12. Microwave match characteristics (return loss) of four-element TWDA at 5-V reverse bias. Return loss is shown for both ports of the detector array.

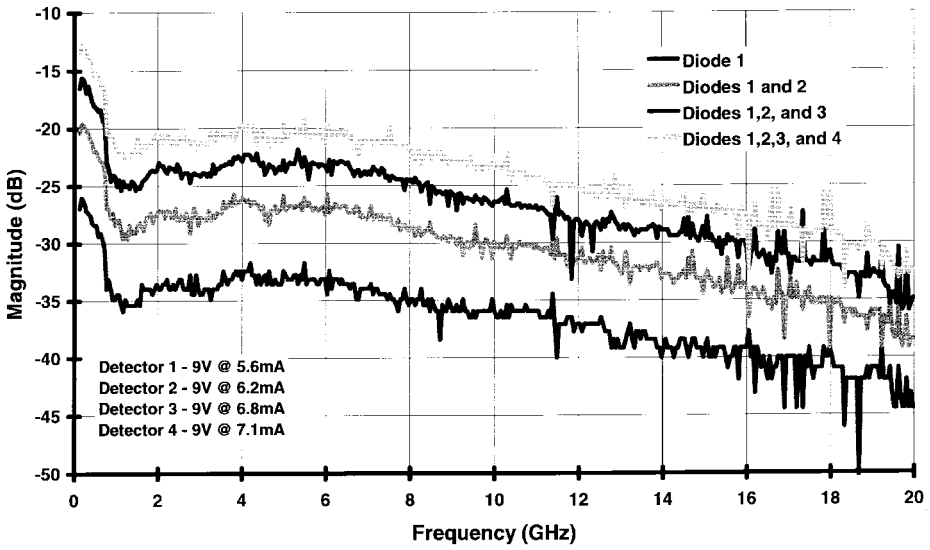

Fig. 13. Fiber-optic link insertion gain versus frequency for a four-element TWDA. Responses are for one, two, three, and all four of the detectors optically excited.

both an excellent heat conduction path as well as a reasonable expansion-coefficient match to the InP detectors.

The electrical combining network was constructed using thick-film fabrication techniques. It consisted of an 380-μm-thick alumina substrate with gold high-impedance transmission lines. The gold transmission lines were located very near the edge of the substrate for a short connection to the detectors. Extremely short bondwires connected to the photodetectors to the high impedance lines. The use of a printed interconnect circuit eliminates much of the variability in the circuit construction previously encountered with the bondwire interconnects.

The close proximity of the transmission line to the substrate edge has a substantial impact on the line impedance and phase velocity. The transmission line was a 100-μm-wide line which was located 75 μm from the edge of the substrate. Electromagnetic simulations using a quasi-static solver yielded an effective line impedance of approximately 97 Ω and an effective microwave index of 2.06. DeLoach measurements show the detectors exhibited a junction capacitance of approximately 0.15–0.2 pF and a effective series resistance of approximately 8–10 Ω. The impedance and phase velocity of the high impedance line were used to calculate appropriate line lengths between each of the photodetectors to yield a 50-Ω characteristic impedance for the artificial transmission line. Optical fibers were coupled to the individual detectors resulting in responsivities greater than 0.8 A/W. The completed four-element submount was mounted in a 18-GHz test fixture, as shown in Fig. 11.

D. Four-Element TWDA Results

The measured return-loss characteristics of the input and output ports of the four-element photodiode array (with no optical input) are shown in Fig. 12. A photodetector bias of 9 V was applied through an external bias tee. The return loss of the artificial transmission line and fixturing was better than

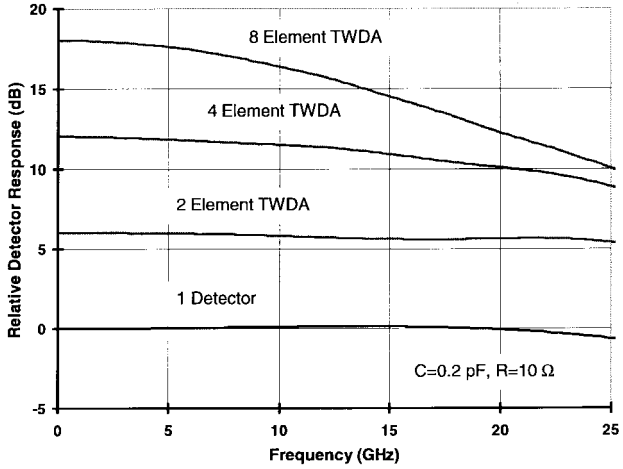

Fig. 14. Ideal TWDA detector response for a one-, two-, four-, and eight-element detector array using $C_d = 0.2$ pF and $R_s = 10\ \Omega$.

14 dB from 0.13 GHz to $>$ 18 GHz, again indicating a good impedance match to the photodetector array.

A test setup similar to that shown in Fig. 7 was used to test the four-element TWDA. In these experiments, the optical attenuators were removed (as equal photocurrents are not required). The two-way optical splitter was replaced with a four-way splitter to provide the proper number of optical outputs. Optical input power to each of the detectors ranged from 6 to 10 mW, resulting in photocurrents on the order of 5–8 mA. The insertion phase of each detector in the network was measured individually and the optical time delays were adjusted to equalize all four path lengths. The propagation delay between the individual detectors was approximately 12 ps.

The measured insertion loss of the four-element TWDA is shown in Fig. 13. This graph demonstrates the insertion-loss improvement as first one, then two, three, and four detectors are activated in the circuit. As expected, a 13-dB improvement in insertion loss is realized as the operating photocurrent goes

from 5.6 mA (a single detector) to 26 mA (all four detectors). All measured fiber-link responses are actual link insertion loss from modulator input to detector output.

Observation of the insertion loss responses shows a notable rolloff in insertion loss as a function of frequency. A good portion of this rolloff is due to the characteristics of the electro-optic modulator. However, some of this rolloff is also due to the detector array itself. Circuit simulations using Super-Compact demonstrate that the detector array rolloff is due to the effective series resistance exhibited by the detectors. These simulations are performed by replacing the detectors in a detector array with their equivalent current sources, capacitors, and series resistors, as shown in Fig. 2. The results of simulations for ideal TWDA detector responses with various numbers of detectors possessing 0.2-pF junction capacitance and 10-Ω resistance are shown in Fig. 14. It is apparent that as the number of detectors increases, so does the dissipated energy at high frequencies. This rolloff response presents a practical limitation to the number of detectors which can be arrayed in a coherent detector network.

The detector network losses associated with the distribution and delay of optical signals to each of the four detectors consists of the excess insertion loss of the four-way optical-power divider and the propagation losses of the fiber feeds and delays. The excess loss of a fused-fiber four-way splitter is approximately 0.3 dB. The insertion loss of the single-mode optical fiber which makes up the interconnects and the optical delays paths is negligible. In later experiments, the optical-feed network was replaced by one consisting of a fused four-way fiber splitter with output fibers tailored to the appropriate delays. This detector array exhibited an effective responsivity of approximately 0.7 A/W, including splitter excess loss. Utilizing fiber for the interconnects and power splitters presents significantly lower losses than those associated with semiconductor waveguides and power splitters. This is essential for low-loss high-efficiency detector networks, especially when working with high optical-power levels.

IV. Conclusion

A TWDA constructed using two commercial 75-μm-diameter InGaAs photodiodes has achieved four times the RF output of a single detector with an excellent return loss ($>$15 dB) over a bandwidth of greater than 10 GHz. The inductance required to produce this 50-Ω quasi-transmission line was obtained using detector bondwires of tailored length. The 6-dB increase in RF output level was obtained by coherently combining the currents from two equally illuminated detectors, fed by properly delayed optical signals.

A second TWDA with four photodetectors has achieved greater than 13-dB improvement in RF output signal by using coherent combining of photocurrents. This array exhibited excellent return loss ($>$ 15 dB) and operated up through 18 GHz. This array utilized metal detector submounts and was interconnected with high-impedance transmission lines for more reproducible performance. The two- and four-element TWDA networks demonstrate the ability to combine the output of multiple photodetectors in a traveling-wave arrangement while retaining their bandwidth.

Future work will emphasize integration of the transmission lines and photodetectors using hybrid and eventually monolithic techniques. Currently, discrete passive optical-fiber components and hand-cleaved custom-length fibers are being used to implement the optical-feed network. Ultimately, integrated-glass optical-waveguide splitters and delay lines will enable a single low-loss fiber connection to a network having N individual detectors. Such a device may produce N^2 times the RF output signal and yet retain the bandwidth and simple packaging of a single detector.

Acknowledgment

The authors thank D. Mockler for technician support, and M. Avery and J. Baumann for help in building the precision fiber-cleaving apparatus. The authors also acknowledge the contributions of B. Kanack during the early stages of TWDA development.

References

[1] H. F. Taylor, O. Eknoyan, C. S. Park, K. N. Choi, and K. Chang, "Traveling wave photodetectors," *Proc. SPIE–Int. Soc. Opt. Eng.*, vol. 1217, pp. 59–63, 1990.

[2] K. S. Giboney, M. J. W. Rodwell, and J. E. Bowers, "Traveling-wave photodetectors," *IEEE Photon. Technol. Lett.*, vol. 4, pp. 1363–1365, Dec. 1992.

[3] K. S. Giboney, L. N. Radhakrishnan, T. E. Reynolds, S. T. Allen, R. P. Mirin, M. J. W. Rodwell, and J. E. Bowers, "Travelling-wave photodetectors with 172-GHz bandwidth and 76-GHz bandwidth-efficiency product," *IEEE Photon. Technol. Lett.*, vol. 7, pp. 412–414, Apr. 1995.

[4] V. M. Hietala, G. A. Vawter, T. M. Brennan, and B. E. Hammons, "Traveling-wave photodetectors for high-power, large bandwidth applications," *IEEE Trans. Microwave Theory Tech.*, vol. 43, pp. 2291–2298, Sept. 1995.

[5] M. C. Wu, L. Y. Lin, and T. Itoh, "A new ultrafast photodetector: Optical-to-microwave transformer," in *OE/LASE '94 Symp. Generation, Amplification, Measurement of Ultrashort Laser Pulses*, Los Angeles, CA, January 22–29, 1994, pp. 228–236.

[6] L. Y. Lin, M. C. Wu, T. Itoh, T. A. Vang, R. E. Muller, D. L. Sivco, and A. Y. Cho, "Velocity matched distributed photodetectors with high-saturation power and large bandwidth," *IEEE Photon. Technol. Lett.*, vol, 8, pp. 1376–1378, Oct. 1996.

[7] C. L. Goldsmith and R. Magnusson, "Bandwidth improvements for loaded-line traveling wave electro-optic modulators," in *IEEE Microwave Theory Tech. Symp.*, Orlando, FL, May 1995, pp. 1499–1502.

[8] C. L. Goldsmith and B. Kanack, "Broad-band microwave matching of high speed photodiodes," in *IEEE Microwave Theory Tech. Symp.*, Atlanta, GA, June 1993, pp. 233–236.

[9] K. J. Williams, "Nonlinear mechanisms in microwave photodetectors operated with high intrinsic region electric fields," *Appl. Phys. Lett.*, vol. 65, no. 10, pp. 1219–1221, Sept. 1994.

[10] K. J. Williams, R. D. Esman, and M. Dagenais, "Effects of high space-charge fields on the response of microwave photodetectors," *IEEE Photon. Technol. Lett.*, vol. 6, pp. 639–641, May 1994.

Charles L. Goldsmith (S'79–M'80–SM'94) received the B.S. and M.S. degrees in electrical engineering from the University of Arizona, Tucson, in 1980 and 1982, respectively, and the Ph.D. degree in electrical engineering from the University of Texas at Arlington, in 1995.

In 1986, he joined Texas Instruments RF/Microwave Laboratory, Dallas, TX, where he has participated in the design and development of broad-band microwave components and subsystems in the 1–60 GHz frequency range. In recent years, his research interests have led to design and construction of low-loss fiber-optic links for phased-array applications and the development of micromechanical microwave switches for low-cost radar applications.

Dr. Goldsmith is a senior member of the IEEE Microwave Theory and Techniques Society, IEEE Lasers and Electro-optics Society, and a member of the Optical Society of America, and Tau Beta Pi.

Gregory A. Magel (S'80–M'81) received the B.S. degree in electrical engineering from Rice University, Houston, TX, in 1981, and the M.S. and Ph.D. degrees from Stanford University, Stanford, CA, in 1983 and 1990, respectively.

He is a Technical Staff Member in the Photonics & Micromaching Branch of Texas Instruments Corporate Research & Development, Dallas, TX. His research interests include micromechanical integrated-optic and fiber-optic switches, optical interconnects, and analog microwave fiber-optic devices and systems.

Dr. Magel is a member of the Optical Society of America, IEEE Lasers and Electro-optics Society, Tau Beta Pi, Phi Beta Kappa, Sigma Pi Sigma, and Eta Kappa Nu.

Richard J. Baca (M'97) received the B.S. degree in electrical engineering from Texas A&M University, College Station, in 1988, and the M.S. and Ph.D. degrees from the University of Illinois, Urbana, in 1991 and 1996 respectively.

In 1996, he joined Texas Instruments Incorporated. He has been involved in the design and development of low-loss microwave to fiber-optic links. His research interests are in the area of fiber-optic communications systems.

Dr. Baca is a member of the IEEE Lasers and Electro-optics Society and the Society of Hispanic Professional Engineers.